ARTHRITIS & RHEUMATOLOGY
Vol. 68, No. 4, April 2016, pp 1026–1038
DOI 10.1002/art.39481

The Role of Follicular Helper T Cell Molecules and Environmental Influences in Autoantibody Production and Progression to Inflammatory Arthritis in Mice

Nina Chevalier,[1] Laurence Macia,[2] Jian K. Tan,[3] Linda J. Mason,[3] Remy Robert,[3] Alison N. Thorburn,[3] Connie H. Y. Wong,[3] Louis M. Tsai,[3] Katherine Bourne,[4] Robert Brink,[4] Di Yu,[3] and Charles R. Mackay[3]

Objective. **Antibody-mediated autoimmunity involves cognate interactions between self-reactive T cells and B cells during germinal center (GC) reactions. The aim of this study was to determine the role of essential follicular helper T (Tfh) cell molecules (CXCR5, signaling lymphocytic activation molecule–associated protein) on autoreactive CD4+ cells and the role of certain environmental influences that may determine GC-driven autoantibody production and arthritis development.**

Methods. **We transferred self-reactive CD4+ cells from KRN-Tg mice into recipient mice, which induced autoantibodies and autoinflammatory arthritis. This model allowed manipulation of environmental effects, such as inflammation, and use of transferred cells that were genetically deficient in important Tfh cell–associated molecules.**

Results. **A deficiency of signaling lymphocytic activation molecule–associated protein (SAP) in CD4+ cells from KRN-Tg mice completely protected against arthritis, indicating that stable T cell–B cell interactions are required for GC formation, autoantibody production, and arthritis induction. In contrast, a CXCR5 deficiency in CD4+ cells from KRN-Tg mice still induced disease when these cells were transferred into wild-type mice, suggesting that T cell help for B cells could rely on other migration mechanisms. However, various manipulations influenced this system, including elimination of bystander effects through use of $CD28^{-/-}$ recipient mice (reduced disease) or use of inflammation-inducing Freund's complete adjuvant (progression to arthritis). We also examined the capacity of preexisting GCs with a nonautoimmune specificity to co-opt autoimmune T cells and observed no evidence for any influence.**

Conclusion. **In addition to the quality and quantity of cognate CD4+ cell help, external factors such as inflammation and noncognate CD4+ cell bystander activation trigger autoimmunity by shaping events within autoimmune GC responses. SAP is an essential molecule for autoimmune antibody production, whereas the importance of CXCR5 varies depending on the circumstances.**

Germinal centers (GCs) are structures within lymphoid tissue wherein B cells undergo clonal expansion, class-switch recombination, and affinity maturation (1). GC formation depends on cognate interactions between antigen-specific B cells, CD4+ cells, and dendritic cells (DCs). Among effector CD4+ cells, follicular helper T (Tfh) cells provide T cell help to B cells and

Supported by the National Health and Medical Research Council of Australia (grant to Dr. Mackay). Dr. Chevalier's work was supported by the DFG (awards CH 818/1-1 and CH 818/1-2) and the Fritz Thyssen Foundation (award 20.13.0.114).

[1]Nina Chevalier, MD: University Medical Centre Freiburg, Freiburg, Germany, Monash University, Clayton Campus, Melbourne, Victoria, Australia, and Garvan Institute of Medical Research, Sydney, New South Wales, Australia; [2]Laurence Macia, PhD: Monash University, Clayton Campus, Melbourne, Victoria, Australia, and Charles Perkins Centre, University of Sydney, Camperdown, New South Wales, Australia; [3]Jian K. Tan, BSc, Linda J. Mason, Remy Robert, PhD, Alison N. Thorburn, PhD, Connie H. Y. Wong, PhD, Louis M. Tsai, PhD, Di Yu, PhD, Charles R. Mackay, PhD (current address: Pfizer Inc., Cambridge, Massachusetts): Monash University, Clayton Campus, Melbourne, Victoria, Australia; [4]Katherine Bourne, BSc, Robert Brink, PhD: Garvan Institute of Medical Research, Sydney, New South Wales, Australia.

Dr. Mackay has received consulting fees from Pfizer (more than $10,000) and is currently employed by Pfizer; he also owns stock or stock options in G2 Therapies.

Address correspondence to Nina Chevalier, MD, Department of Rheumatology and Clinical Immunology, University Medical Center Freiburg, Hugstetter Strasse 55, 79106 Freiburg, Germany (e-mail: nina.chevalier@uniklinik-freiburg.de); or to Charles R. Mackay, PhD, Department of Immunology and Inflammation, Monash University Clayton, Melbourne, Victoria 3088, Australia (e-mail: charles.mackay@monash.edu).

Submitted for publication January 27, 2015; accepted in revised form October 22, 2015.

drive the GC reaction (2–4). Tfh cells are marked by high expression of the chemokine receptor CXCR5, which facilitates their migration to B cell follicles (5–8). Moreover, Tfh cells express a unique combination of transcription factors and effector molecules related to their specialized B cell helper function, including Bcl-6, high levels of costimulatory molecules such as inducible T cell costimulator (ICOS), programmed death 1 (PD-1), the cytokine interleukin-21, and the cytoplasmic adaptor protein signaling lymphocytic activation molecule (SLAM)–associated protein (SAP) (2–4,8). SAP expression on CD4+ cells is important for the generation of GCs by promoting long-lasting mobile conjugate pairs of CD4+ cells with antigen-presenting cognate B cells (9,10). Tfh cells and their associated effector molecules are important in both normal responses and autoantibody-driven autoimmune diseases (1,11–14).

Rheumatoid arthritis (RA) is an autoimmune disease characterized by synovial inflammation and destruction of cartilage and bone. The precise underlying immunopathologic mechanisms have not yet been completely defined; however, both innate immunity and adaptive immunity play a role, particularly autoantibodies. To date, various RA-associated antibodies have been identified, including the relatively nonspecific rheumatoid factor and anti–citrullinated protein antibodies (ACPAs). Similar to many pathologic autoantibodies, most ACPAs are high-affinity IgG antibodies, indicative of class switching, affinity maturation, and involvement of the GC reaction (1).

In the K/BxN mouse model of arthritis, autoantibody production and GC formation rely on the integrity of follicular DC (FDC) networks, which support recruitment of arthritogenic Tfh cells (12). In one study, a deficiency of the signature Tfh molecule CXCR5 on CD4+ cells from arthritogenic KRN-Tg mice resulted in complete abrogation of GC reactions, autoantibody production, and disease development (12). However, several studies questioned the importance of CXCR5 for CD4+ cell recruitment into B cell follicles and humoral immunity in nonautoimmune settings (15,16). Although some studies showed that CXCR5 was indispensable for T cell entry to B cell follicles and GC formation (12,17), others showed only mildly reduced GC responses under circumstances of T cell–specific CXCR5 deficiency (15,16,18). Moreover, in these latter studies, CXCR5-deficient CD4+ cells were still able to access GCs. The variability in GC formation and antibody production between these studies suggests that factors such as mouse housing differences and background levels of immune stimulation may be influencing progression to disease. External environmental factors are thought to contribute to disease progression in many autoimmune diseases (19).

The aim of this study was to clarify the role of CXCR5 on CD4+ cells for their recruitment to GCs, particularly in an autoimmune setting (the KRN mouse model of arthritis). In addition, we sought to address whether other factors (e.g., the presence of an inflammatory environment, noncognate CD4+ cell bystander effects, and unrelated background GC reactions) affected the GC reaction in KRN mice. Our results showed that noncognate background environmental influences become critical when follicular CD4+ cell recruitment is hampered by CXCR5 deficiency.

MATERIALS AND METHODS

Mice. KRN-Tg C57BL/6 mice were obtained from D. Mathis and C. Benoist. $CXCR5^{-/-}$ and SW_{HEL} mice, $SAP^{-/-}$ mice, and $CD28^{-/-}$ mice were obtained in-house (from RB, ST, and DY, respectively). $B6.H2^{g7/g7}$ mice were purchased from The Jackson Laboratory. NOD/ShiLtJArc mice and CD45.1-congenic C57BL/6 (B6.SJL-ptprc^a) mice were obtained from the Animal Resources Centre (Perth, Australia). $CXCR5^{-/-}$.KRN-Tg and $SAP^{-/-}$.KRN-Tg mice were generated by crossing $CXCR5^{-/-}$ and $SAP^{-/-}$ mice with KRN-Tg mice, respectively; $CD28^{-/-}.A^{g7+/-}$ and $SAP^{-/-}.A^{g7+/-}$ mice were generated by crossing $CD28^{-/-}$ and $SAP^{-/-}$ mice with $B6.H2^{g7/g7}$ mice. Crossing KRN-Tg mice with NOD mice generates arthritic K/BxN ([KRN-Tg × NOD]F1) mice, crossing B6.SJL/ptprc^a mice with NOD mice generates BxN.45.1 ([B6.SJL/ptprc^a × NOD]F1) mice, and crossing C57BL/6 mice with $B6.H2^{g7/g7}$ mice generates B6 × $B6H2^{g7}$ ([C57BL/6 × $B6H2^{g7}$]F1) mice. When indicated, some of the strains were further crossed with B6.SJL/ptprc^a mice to generate CD45.1-congenic or CD45.1.2-congenic mice. Genotypes were assessed by genomic polymerase chain reaction (PCR) or fluorescence-activated cell sorting (FACS). Experiments were approved by the Garvan/St. Vincent's and Monash Animal Ethics Committee. For experiments comparing $CD28^{-/-}.A^{g7+/-}$ mice and BxN.45.1 mice, the mice were housed together for 1 month to exclude effects of distinct commensal microorganisms.

Adoptive transfer experiments, K/BxN serum transfer, and Freund's complete adjuvant (CFA) injection. As previously described (20), cell suspensions were prepared from pooled spleens and lymph nodes (LNs), and CD4+ cells were enriched using MACS MicroBeads (Miltenyi Biotech) and sorted by FACS to >97% purity. Purified CD4+ cells were injected intravenously into recipients. Generally, 1.5×10^6 or 0.75×10^6 CD4+ cells from KRN-Tg mice were injected into BxN.45.1 and B6 × $B6H2^{g7}$ mice or $CD28^{-/-}.A^{g7+/-}$ mice, respectively. Similar to what was described by Victoratos and Kollias (12), recipients received 2.5 Gy irradiation prior to transfer of CD4+ cells from KRN-Tg mice, to enhance engraftment of transferred cells. The use of different cell numbers was based on the assumption that adoptively transferred CD4+ cells from KRN-Tg mice may encounter less competition in a CD28-deficient host due to a T cell receptor–unresponsive endogenous CD4+ compartment as well as a general Treg cell defect in these mice (21).

Hen egg lysozyme (HEL)–binding B cells were isolated from SW_{HEL} mice; generally, a mixture of spleen cells con-

taining 3×10^4 HEL-binding B cells was transferred. Production of HEL^{3x} proteins, their conjugation to sheep red blood cells (SRBCs), and adoptive transfer have been described previously (22,23). Serum was collected from 8-week-old K/BxN mice, and arthritis was induced by a 150-μl intraperitoneal injection of K/BxN mouse serum on days 0 and 2. CFA and phosphate buffered saline (PBS) were mixed at a 1:1 ratio, and 200 μl was injected intraperitoneally.

Arthritis scoring. The clinical severity of arthritis was scored as previously described (20). All 4 paws were scored based on a scale of 0 to 3, and severity was described as the cumulative score.

Flow cytometric analysis, anti–glucose-6-phosphate isomerase (anti-GPI) enzyme-linked immunosorbent assay (ELISA), real-time quantitative PCR, and immunofluorescence analysis. For flow cytometry, cells were collected from crushed peripheral LNs (pooled inguinal, brachial, axillary, and cervical) or spleens and stained with antibodies to ICOS, CD44, CD45.1, CD95 (all from eBioscience), CD45.2, GL7, IgG1, and CXCR5 (all from BD Biosciences). Anti-GPI IgG1 levels in serum were determined by ELISA, as previously described (20). The titer was calculated as $\log_2$ of the last dilution factor for which the optical density was 3 times that of background. Total RNA extraction, complementary DNA reverse transcription, and quantitative real-time PCR were performed as previously described (20).

Cryostat sections (6–8 μm) of OCT-embedded spleens were air-dried, fixed in acetone, and rehydrated in PBS. Sections were incubated for 1 hour at room temperature with the following primary antibodies: Alexa Fluor 647–conjugated anti-IgD, Alexa Fluor 488–conjugated anti-CD45.2 (both from BioLegend), biotin-conjugated anti-GL7 (eBioscience), biotin-conjugated anti-CD35, biotin-conjugated anti-CD45.2, and purified anti-CD3 (all from BD Biosciences). Biotinylated antibodies were detected with streptavidin–Alexa Fluor 555 (Invitrogen) or streptavidin–allophycocyanin (eBioscience), and CD3 was detected with Alexa Fluor 488–conjugated anti–Armenian hamster IgG. To stain HEL-

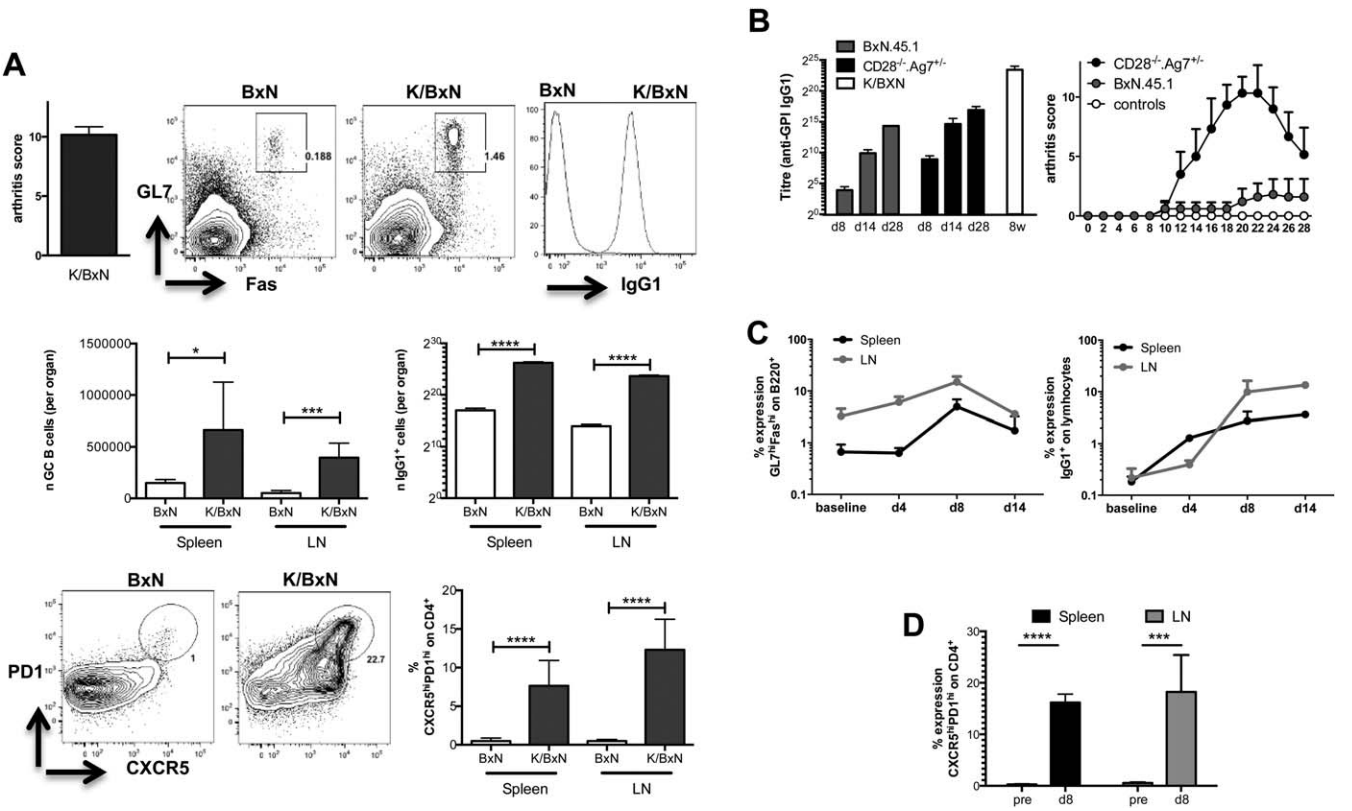

Figure 1. Germinal center (GC) and follicular helper T (Tfh) cell responses are increased in K/BxN mice and after transfer of arthritis-inducing CD4+ cells from KRN-Tg mice. **A,** Clinical arthritis scores in K/BxN mice, expression of $GL7^{high}Fas^{high}$ and IgG1 on B220+ B cells, and expression of $CXCR5^{high}PD\text{-}1^{high}$ on CD4+ cells, as determined by fluorescence-activated cell sorting (FACS), in spleens and lymph nodes (LNs) from 8-week-old arthritic K/BxN mice and nonarthritic BxN mice (n = more than 5 per group). **B,** Transfer of CD4+ cells from KRN-Tg mice into BxN.45.1 mice or control BL6 mice and $CD28^{-/-}.A^{g7+/-}$ mice or control $CD28^{-/-}.Ag7^{-/-}$ mice (n = 4–5 per group). Left, Anti–glucose-6-phosphate isomerase (anti-GPI) IgG1 titers in serum on days 8, 14, and 28 after transfer, as measured by enzyme-linked immunosorbent assay. Right, Clinical arthritis scores over time. **C** and **D,** Transfer of CD4+ cells from KRN-Tg mice into BxN.45.1 mice (n = 4–5 per group). Shown are $GL7^{high}Fas^{high}$ expression on B220+ B cells (left) and IgG1+ expression on lymphocytes (right) over time (**C**) and differentiation of transferred $CD45.2^+$ CD4+ cells into $CXCR5^{high}PD\text{-}1^{high}$ Tfh cells on day 8 in spleen and LNs, as determined by FACS analysis (**D**). Also shown are baseline levels in untreated BxN45.1 mice (**C**) and the phenotype of CD4+ cells from KRN-Tg mice (**D**) (n = 5 mice). Values are the mean ± SD. * = $P < 0.05$; *** = $P < 0.001$; **** = $P < 0.0001$. PD-1 = programmed death 1; pre = phenotype of naive CD4+ cells from KRN-Tg mice before transfer.

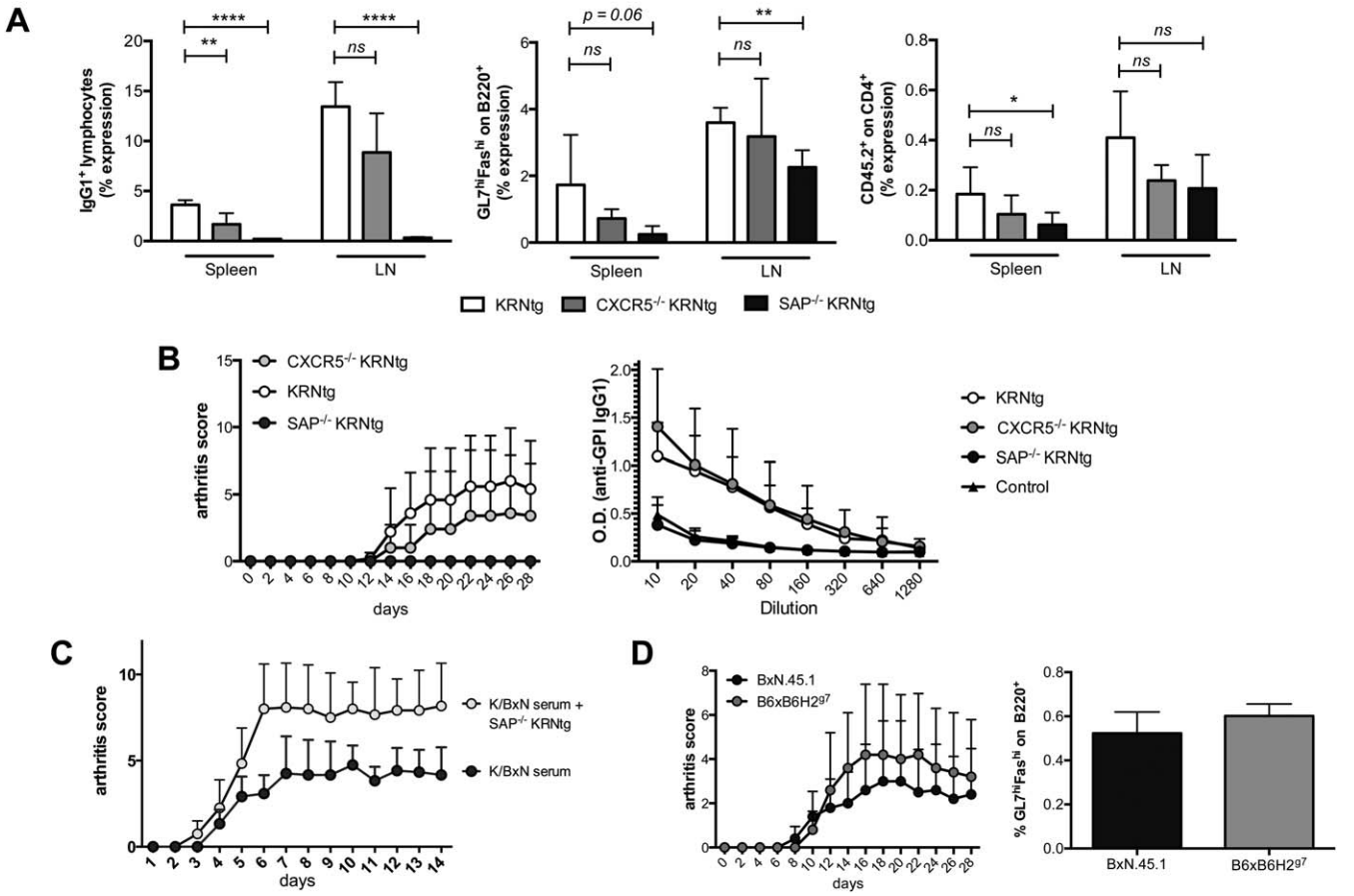

Figure 2. Relative importance of signaling lymphocytic activation molecule–associated protein (SAP) versus CXCR5 for anti–GPI responses and inflammatory arthritis. **A** and **B,** Transfer of CD4+ cells from CD45.2$^+$ KRN-Tg, CXCR5$^{-/-}$.KRN-Tg, or SAP$^{-/-}$.KRN-Tg mice into CD45.1$^+$ BxN.45.1 mice. Shown are the percentage of IgG1+ lymphocytes (left), expression of GL7^{high}Fas^{high} on B220+ cells (middle), and percentage of recovered transferred CD45.2$^+$ CD4+ cells (right) on day 8 after transfer, as determined by FACS analysis (n = 4–5 mice per group) (**A**) and clinical arthritis scores over time (left) and anti-GPI IgG1 expression in serum as measured by enzyme-linked immunoassay in serum on day 14 after transfer (right) (n = 4–5 mice per group) (**B**). **C,** Induction of arthritis in BxN.45.1 mice by intraperitoneal injection of 150 μl K/BxN mouse serum on days 0 and 2, with one group receiving CD4+ cells from SAP$^{-/-}$.KRN-Tg mice on day 0. Shown are clinical arthritis scores over time. **D,** Transfer of CD4+ cells from CXCR5$^{-/-}$.KRN-Tg mice into BxN.45.1 or B6 × B6H2^{g7} mice. Shown are clinical arthritis scores over time (left) and GL7^{high}Fas^{high} expression on B220+ cells on day 8 after transfer (right). Values are the mean ± SD. $* = P < 0.05$; $** = P < 0.01$; $**** = P < 0.0001$. NS = not significant (see Figure 1 for other definitions).

binding cells, sections were incubated with 200 ng/ml HEL (Sigma-Aldrich), polyclonal rabbit anti-HEL sera (Rockland), and Alexa Fluor 488–conjugated goat anti-rabbit IgG or phycoerythin-conjugated goat anti-rabbit IgG (Invitrogen).

Statistical analysis. *P* values were calculated by unpaired *t*-test, using Instat software (GraphPad). Data are expressed as the mean ± SD and are representative of at least 2 independent experiments. *P* values less than or equal to 0.05 were considered significant.

RESULTS

Increased GC and Tfh cell responses in arthritic KRN mice. Arthritis development in the KRN mouse model is mediated by CD4+ cells from KRN-Tg mice that recognize peptides 281–293 of the ubiquitously expressed enzyme GPI in the context of the NOD-specific major histocompatibility complex class II molecule, I-A^{g7}. Previous studies indicated that activated CD4+ cells from KRN-Tg mice could adopt a Tfh phenotype (12,20) that may contribute to the expansion of GPI-specific B cells and anti-GPI IgG1 production, which precipitates disease in the joints (24,25).

First, we used an adoptive transfer strategy to examine whether Tfh cell differentiation correlates with induction of GCs, GPI-specific IgG1, and inflammatory arthritis in K/BxN mice. Transfer of gene-deficient CD4+ cells from KRN-Tg mice allowed an analysis of the relevance of Tfh molecules on autoreactive CD4+

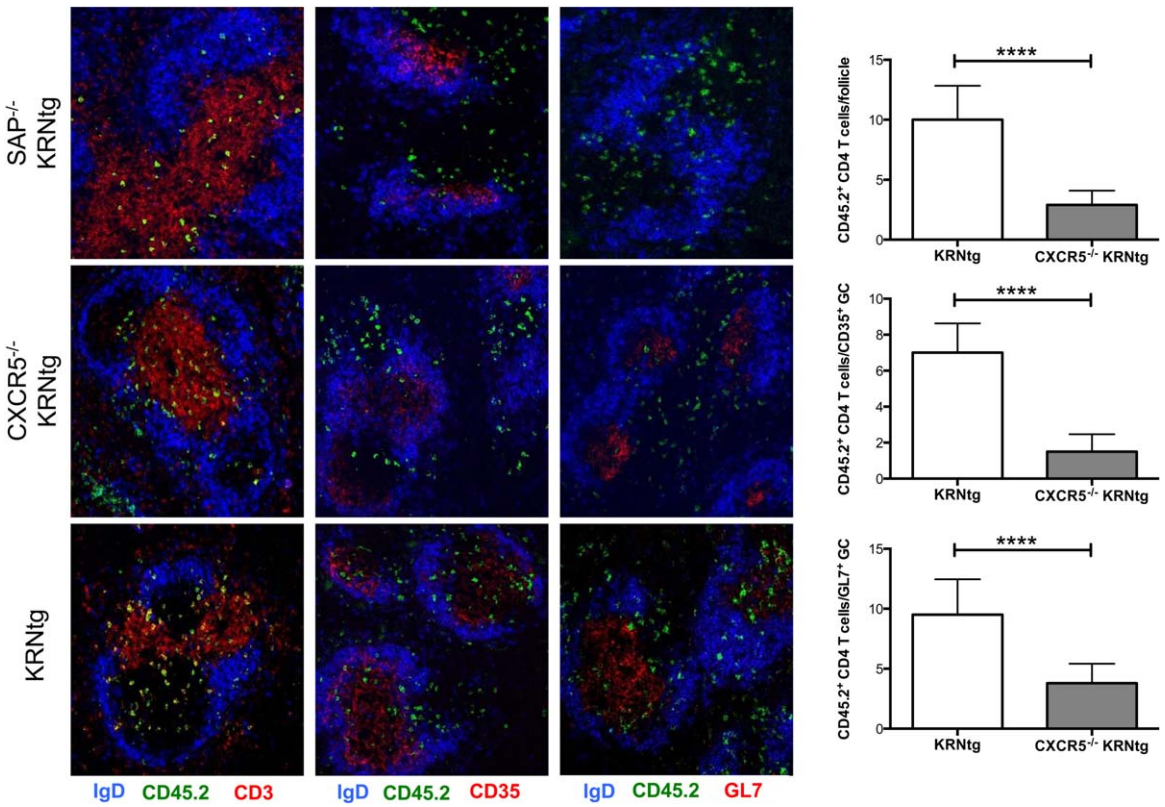

Figure 3. Relative importance of signaling lymphocytic activation molecule–associated protein (SAP) versus CXCR5 for germinal center (GC) formation and follicular CD4+ cell migration. CD4+ cells from CD45.2$^+$ KRN-Tg, CXCR5$^{-/-}$.KRN-Tg, or SAP$^{-/-}$.KRN-Tg mice were transferred into CD45.1$^+$ BxN.45.1 mice. Left, Immunofluorescence staining of spleens 8 days after transfer shows localization of follicular dendritic cell networks (anti-CD35–stained [red]), B cell follicles (anti-IgD–stained [blue]), GCs (anti-GL7–stained [red]), T cell zone (anti-CD3–stained [red]), and adoptively transferred cells (anti-CD45.2–stained [green]). Original magnification × 10. Right, Enumeration of adoptively transferred CD45.2$^+$ BxN.45.1 cells per follicle (top), per CD35+ GC (middle), and per GL7+ GC (bottom) from 10–12 follicles of equivalent size (n = 3–5 mice per group). Values are the mean ± SD. **** = $P < 0.0001$.

cells. Moreover, the transfer strategy allowed us to manipulate the recipient animal in order to study background environmental influences.

In arthritic K/BxN mice, GC responses (GL7^{high}Fas^{high} expression on GC B cells) and IgG1 class switching were highly increased in spleens and LNs (Figure 1A). This was in accordance with high anti-GPI IgG1 serum levels (Figure 1B), robust disease induction (Figure 1A), and high CXCR5 and PD-1 expression levels on CD4+ cells, which are characteristic of Tfh cells (Figure 1A). Adoptive transfer of CD4+ cells from KRN-Tg mice into BxN.45.1 recipients significantly induced formation of GC B cells, which peaked on day 8, and robust IgG1 class switching (Figure 1C). This also correlated with the adoption of a CXCR5^{high}PD-1^{high} Tfh phenotype (Figure 1D) (20). GPI-specific IgG1 was detectable beginning 8 days after transfer (Figure 1B), and disease onset was detectable beginning approximately 8–10 after transfer and thereafter (Figure 1B). Generally, anti-GPI IgG1 titers and disease scores observed using the adoptive transfer strategy (Figure 1B) were lower than those in K/BxN mice (Figures 1A and B). We assume that these differences may be attributable to numerical underrepresentation and homeostatic out-proliferation of transferred CD4+ cells from KRN-Tg mice by endogenous CD4+. Taken together, these results underscore the importance of Tfh cells and the GC reaction for autoantibody production and disease development in the KRN mouse model of arthritis.

Relative importance of SAP versus CXCR5 for anti-GPI responses and inflammatory arthritis. To assess the importance of individual molecules for Tfh cell–mediated GC B cell responses, autoantibody production, and disease development, we performed adoptive transfer experiments using CD4+ cells from CXCR5$^{-/-}$.KRN-Tg and SAP$^{-/-}$.KRN-Tg mice. Transfer of CD4+ cells from SAP$^{-/-}$.KRN-Tg mice into BxN.45.1 recipients failed to give rise to any GCs or

IgG1 class switching (Figure 2A). Also, there was no production of anti–GPI–specific IgG1, and arthritis development was undetectable when CD4+ cells from $SAP^{-/-}$. KRN-Tg mice were transferred (Figure 2B). Transfer of CD4+ cells from $CXCR5^{-/-}$.KRN-Tg mice, however, did not result in complete abrogation of these parameters (Figures 2A and B). Compared with adoptively transferred CD4+ cells from wild-type (WT) KRN-Tg mice, the magnitude of GC formation, IgG1 class switching, and disease development were, however, reduced (Figures 2A and B). The recovery of adoptively transferred CD4+ cells from $CXCR5^{-/-}$.KRN-Tg and $SAP^{-/-}$.KRN-Tg mice was lower than that seen for CD4+ cells from WT KRN-Tg mice (Figure 2A).

GC formation by CD4+ cells from $CXCR5^{-/-}$. KRN-Tg or WT KRN-Tg mice, versus GC deficiency with CD4+ cells from $SAP^{-/-}$.KRN-Tg mice, was also confirmed in situ by immunohistology (Figure 3). Moreover, we examined the localization of adoptively transferred CD4+ cells based on CD45.2 expression. Interestingly, CD4+ cells from $CXCR5^{-/-}$.KRN-Tg mice could be detected within follicular GCs, although the frequency was significantly lower than that of CD4+ cells from WT KRN-Tg mice (Figure 3). We also observed that localization of transferred CD4+ cells from $CXCR5^{-/-}$.KRN-Tg mice overlapped with that of GL7+ GCs as well as CD35+ FDCs, which are prominent in the GC light zone. Compared with transferred CD4+ cells from WT KRN-Tg mice, localization of transferred CD4+ cells from $CXCR5^{-/-}$. KRN-Tg was sparse (Figure 3) but sufficient to induce anti-GPI IgG1 and disease (Figure 2B).

To exclude the possibility that SAP-deficient mouse CD4+ cells exert regulatory functions, we cotransferred serum antibodies and CD4+ cells from $SAP^{-/-}$.KRN-Tg mice (Figure 2C). The augmented disease severity in the presence of CD4+ cells from $SAP^{-/-}$. KRN-Tg mice provides evidence against a suppressive role for SAP after priming and supports a nonhumoral arthritis-promoting role for T cells (26). Thus, the failure to produce arthritis following transfer of CD4+ cells from $SAP^{-/-}$.KRN-Tg mice confirms the necessity of stable T cell–B cell interactions for an efficient GC response and production of disease-inducing autoantibodies (10). The observation that CXCR5 expression was not mandatory for CD4+ cell access into follicular GCs and autoantibody and disease development contrasts with the findings described by Victoratos and Kollias (12) and by Hardtke et al (17) but supports the observations in other studies (15,16,18). Mouse genetic background differences are unlikely to explain the discrepancy between our results and those reported by Victoratos and Kollias (12), because transfer of CD4+ cells from $CXCR5^{-/-}$.KRN-Tg mice into B6 × $B6H2^{g7}$ mice versus BxN.45.1 mice induced comparable disease scores and percentages of GCs (Figure 2D).

Severely reduced GC development, autoantibody secretion, and arthritis following transfer of CD4+ cells from $CXCR5^{-/-}$.KRN-Tg mice into $CD28^{-/-}$ recipient mice. As discussed previously, the inconsistent results between studies may be attributable to bystander effects of unrelated immune responses originating from the constant exposure of an organism to environmental influences. Because recent studies suggested that activated noncognate CD4+ cells contribute to the induction of GCs (27), we used $CD28^{-/-}$ mouse recipients for our adoptive transfer strategies in order to test potential bystander effects from noncognate CD4+ cells. Because CD28 represents the main T cell costimulatory receptor, its deficiency imparts limited CD4+ cell activation upon antigenic stimulation. Moreover, $CD28^{-/-}$ mice display impaired GC and antibody responses (28,29). Thus, nonimmunized $CD28^{-/-}$ mice were almost completely devoid of background GCs compared with BxN.45.1 mice, and CD4+ cells from $CD28^{-/-}$ mice expressed significantly reduced levels of the activation marker CD44 (Figure 4A).

As previously observed (20), adoptive transfer of CD4+ cells from KRN-Tg mice into $CD28^{-/-}$.$A^{g7+/-}$ mice resulted in Tfh cell differentiation (Figure 4B). This correlated with GC induction, IgG1+ class switching (Figure 4B), and arthritis (Figures 1B and 4C). Generally, both anti-GPI IgG1 levels and disease scores were higher in $CD28^{-/-}$.$A^{g7+/-}$ mice compared with BxN.45.1 recipients (Figure 1B). We assume that this difference may be attributable to reduced competition by a defective Treg and hypoproliferative T cell compartment and delayed Treg cell/Teff cell expansion of transferred CD4+ cells from KRN-Tg mice into $CD28^{-/-}$ mice (20).

Interestingly, when CD4+ cells from $CXCR5^{-/-}$. KRN-Tg mice were transferred into $CD28^{-/-}$.$A^{g7+/-}$ recipients, we observed an effect opposite to the effect of transfer of CD4+ cells from KRN-Tg mice, because levels of anti-GPI IgG1, arthritis scores, and IgG1+ and GC B cells were significantly reduced (Figure 4C). Moreover, significantly fewer transferred CD4+ cells from $CXCR5^{-/-}$. KRN-Tg mice could be recovered, compared with cells from KRN-Tg mice (Figure 4C); in addition, recovery of transferred CD4+ cells from $CXCR5^{-/-}$.KRN-Tg mice was affected much more in $CD28^{-/-}$.$A^{g7+/-}$ mice (Figure 4C) compared with BxN.45.1 mice (Figure 2A), and the level was too low to allow for localization studies by immunohistology (data not shown).

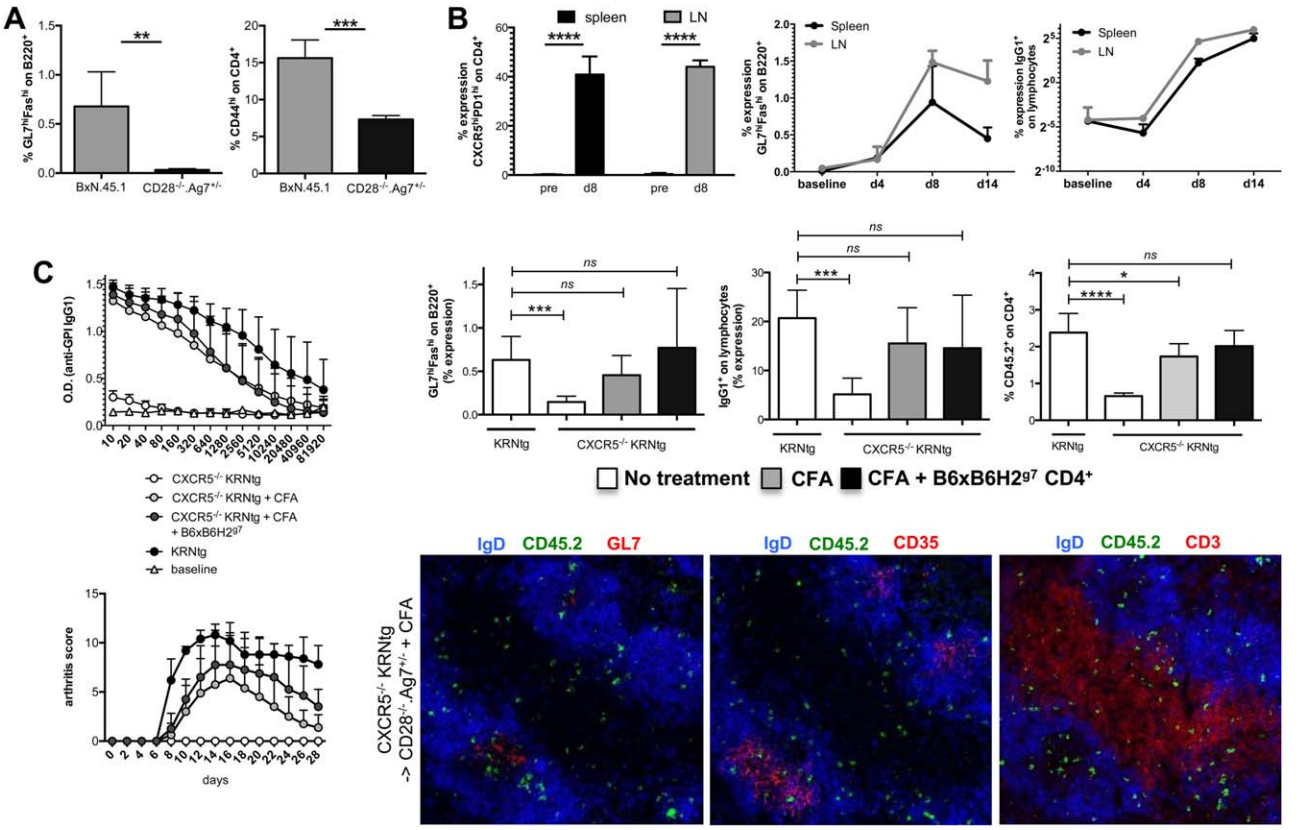

Figure 4. Germinal center development, autoantibody secretion, and arthritis are severely reduced upon transfer of CD4+ cells from CXCR5$^{-/-}$. KRN-Tg mice into CD28$^{-/-}$ recipient mice but can be restored by treatment with Freund's complete adjuvant (CFA). **A,** Percentage of splenic GL7^{high}Fas^{high} expression on splenic B220+ cells (left) and CD44^{high} CD4+ cells in co-housed naive BxN.45.1 mice and CD28$^{-/-}$.A$^{g7+/-}$ mice (right) (n = 5 mice per group). **B,** Transfer of CD4+ cells from KRN-Tg mice into CD28$^{-/-}$.A$^{g7+/-}$ mice (n = 4–5 mice per group). Shown are the differentiation of transferred CD45.2^{+} CD4+ cells into CXCR5^{high}PD-1^{high} follicular helper T cells on day 8 in spleen and lymph nodes (LNs) and time courses of GL7^{high}Fas^{high} B220+ cells, and IgG1+ lymphocytes 4, 8, and 14 days after transfer. **C,** Transfer of CD4+ cells from CD45.2^{+} KRN-Tg or CXCR5$^{-/-}$.KRN-Tg mice into CD45.1^{+} CD28$^{-/-}$.A$^{g7+/-}$ recipients with or without CFA and with or without CD4+ cells from CD45.1.2^{+} B6 × B6H2^{g7} mice (n = 4 mice per group). Left, Anti-GPI IgG1 expression (top) and clinical arthritis scores (bottom) over time. Right, top, Expression of GL7^{high}Fas^{high} on B220+ cells, IgG1+ on lymphocytes, and CD45.2^{+} on CD4+ cells. Bottom, Immunofluorescence staining of spleens from CD28$^{-/-}$.A$^{g7+/-}$ mice 8 days after transfer of CD4+ cells from CXCR5$^{-/-}$.KRN-Tg mice and CFA treatment shows localization of GCs (anti-GL7–stained [red]), follicular dendritic cells (anti-CD35–stained [red]), B cell follicles (anti-IgD–stained [blue]), T cell zone (anti-CD3–stained [red]), and transferred cells (anti-CD45.2–stained [green]). Original magnification × 10. Values are the mean ± SD. * = $P < 0.05$; ** = $P < 0.01$; *** = $P < 0.001$; **** = $P < 0.0001$. NS = not significant (see Figure 1 for other definitions).

Thus, CD28$^{-/-}$.A$^{g7+/-}$ mice displayed severely impaired recruitment of CD4+ cells from CXCR5$^{-/-}$. KRN-Tg mice, which resulted in defective development of GCs, autoantibodies, and disease. The conclusion can be drawn that background activation of normal T cells may affect the behavior of autoimmune CD4+ cells.

Adjuvant-induced autoimmunity in CD28$^{-/-}$ mice that received CD4+ cells from CXCR5$^{-/-}$.KRN-Tg mice. To further examine possible noncognate CD4+ cell bystander effects, we sought to determine whether defective autoreactive B cell responses and disease development after transfer of CD4+ cells from CXCR5$^{-/-}$. KRN-Tg mice to CD28$^{-/-}$.Ag7$^{+/-}$ mice could be restored by cotransfer of noncognate CD4+ cells from CD28$^{+/+}$. A$^{g7+/-}$ mice isolated from B6 × B6H2^{g7} mice and an inflammatory milieu induced by CFA injection. Although cotransfer of CD28-sufficient noncognate CD4+ cells failed (data not shown), CFA alone restored the ability of CD4+ cells from CXCR5$^{-/-}$ KRN-Tg mice to induce GCs, anti-GPI IgG1, and disease in CD28$^{-/-}$.A$^{g7+/-}$ mice and increased their recruitment to the spleen (Figure 4C). Cotransfer of CD4+ cells from CD28$^{+/+}$.A$^{g7+/-}$ mice plus CFA treatment consistently increased these parameters, if only slightly (Figure 4C). Moreover, using immunohistology, we could clearly detect transferred CD4+ cells from CD45.2^{+}CXCR5$^{-/-}$. KRN-Tg mice in follicular GCs (Figure 4C).

These data support the concept that inflammation augments the recruitment of autoreactive CD4+ cells to

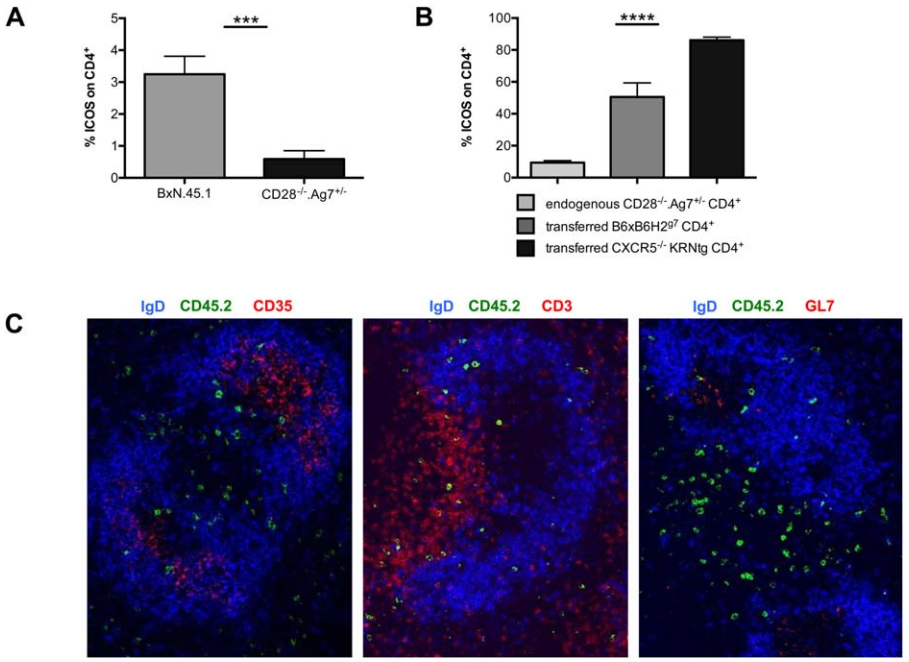

Figure 5. Inducible T cell costimulator (ICOS) levels are increased on CD4+ cells from $CD28^{-/-}$ mice and are further expanded by adjuvant Freund's complete adjuvant (CFA). **A,** Fluorescence-activated cell sorting analysis of splenocytes from co-housed naive BxN.45.1 and $CD28^{-/-}.A^{g7+/-}$ mice (n = 5 mice per group) for expression of ICOS on CD4+ cells. **B,** Adoptive transfer of CD4+ cells from $CD45.2^{+}$ $CXCR5^{-/-}$.KRN-Tg and $CD45.1.2^{+}$ B6 × $B6H2^{g7}$ mice into $CD45.1^{+}$ $CD28^{-/-}.A^{g7+/-}$ recipient mice, with CFA (n = 5 or more mice per group). Expression of ICOS was determined on day 8 after transfer on endogenous and transferred CD4+ cells. **C,** Adoptive transfer of CD4+ cells from $CD45.1^{+}$ $CXCR5^{-/-}$.KRN-Tg and $CD45.2^{+}$ B6 × $B6H2^{g7}$ mice into $CD45.1^{+}$ $CD28^{-/-}.A^{g7+/-}$ mice, with CFA. Immunofluorescence staining of spleens 8 days after transfer shows localization of follicular dendritic cell networks (anti-CD3–stained [red]), B cell follicles (anti-IgD–stained [blue]), GCs (anti-GL7–stained [red]), the T cell zone (anti-CD35–stained [red]), and adoptively transferred cells (anti-CD45.2–stained [green]) (n = 4 mice). Original magnification × 10. Values are the mean ± SD. *** = $P < 0.001$; **** = $P < 0.0001$.

GCs (possibly CXCR5+ and CXCR5−) and restores a defective GC response. The observation that cotransfer of noncognate CD4+ cells from $CD28^{+/+}.A^{g7+/-}$ mice was insufficient to restore the observed deficiencies does not fully rule out their bystander effects, and the insufficiency may be attributable to technical issues such as cell numbers that are too low, inadequate accumulation/positioning in the spleen, or insufficient activation in the absence of CFA. Accordingly, in CFA-treated mice, cotransferred CD4+ cells from $CD28^{+/+}.A^{g7+/-}$ mice had slightly enhancing effects. However, these effects were very weak compared with the strong CFA-induced effects, and these results need to be interpreted with caution and tested by different experimental approaches in future studies.

Regulation of ICOS expression on antigen-nonspecific CD4+ cells by CD28 costimulation and CFA-mediated inflammation. The strong effects of inflammation-inducing CFA are likely multifaceted and probably affect both innate and adaptive immunity. To resume our focus on the possible bystander effects from endogenous noncognate CD4+ cells, we sought to determine which stimuli expressed by CD28-sufficient T cells and CFA might have contributed to the observed effects. Because numerous studies have shown the importance of ICOS–ICOSL for an optimal GC and humoral immune response (30,31) and autoimmunity (32–36), we investigated whether CD28 deficiency and CFA injection affected ICOS expression on CD4+ cells.

Compared with nonimmunized BxN.45.1 mice, nonimmunized $CD28^{-/-}.A^{g7+/-}$ mice displayed significantly reduced ICOS expression on CD4+ cells (Figure 5A). To determine whether CFA induced ICOS expression, we transferred CD4+ cells from $CD45.2^{+}CXCR5^{-/-}$.KRN-Tg mice with noncognate CD4+ cells from $CD45.1.2^{+}$ $CD28^{+/+}.A^{g7+/-}$ mice (isolated from B6 × $B6H2^{g7}$ mice) into $CD45.1^{+}CD28^{-/-}.Ag^{+/-}$ mice. We observed that CFA boosted ICOS expression on both $CD28^{-/-}$ and $CD28^{+/+}$ mouse noncognate CD4+ cells compared with untreated mice (Figure 5B); ICOS expression was highest in antigen-specific CD4+ cells from KRN-Tg mice, and as in untreated mice, noncognate CD4+ cells from $CD28^{+/+}$ mice expressed higher ICOS levels than noncognate CD4+ cells from $CD28^{-/-}$ mice (Figure 5B).

To examine whether transferred noncognate CD4+ cells from $CD45.2^{+}CD28^{+/+}.A^{g7+/-}$ mice also

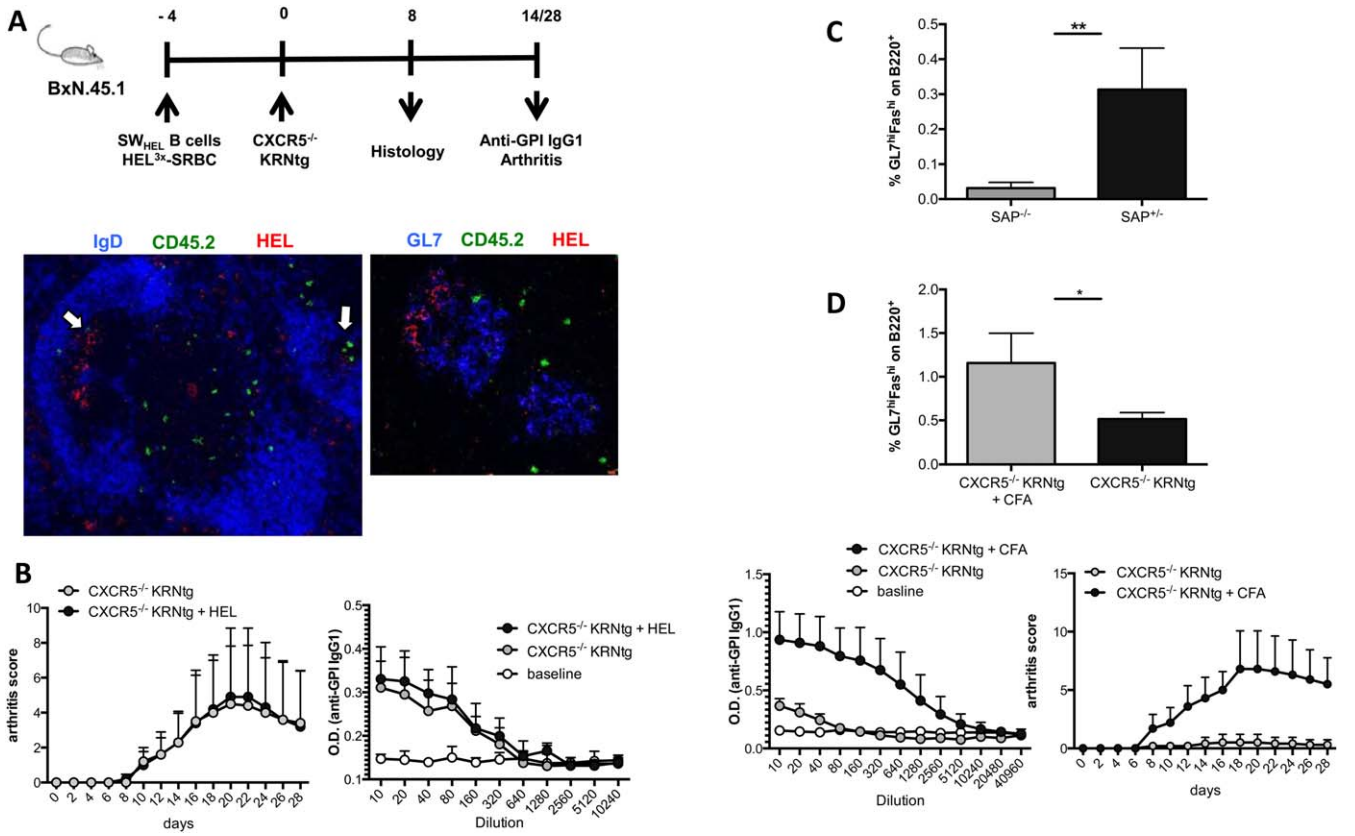

Figure 6. Background germinal centers do not support the development of autoimmunity by co-opting autoaggressive CD4+ cells. **A,** Top, Consecutive transfer and immunization strategy. CD45.1^{+} BxN.45.1 mice received CD45.1^{+} hen egg lysozyme (HEL)–binding SW$_{HEL}$ cells along with sheep red blood cells (SRBCs) conjugated to HEL^{3x} (day −4) followed by CD4+ cells from CD45.2^{+} CXCR5$^{-/-}$.KRN-Tg mice 4 days later (day 0). Bottom, Immunofluorescence staining of spleens 8 days after transfer shows HEL-binding B cells (red), transferred CD4+ cells from CD45.2^{+} CXCR5$^{-/-}$.KRN-Tg mice (green), B cell follicles (IgD [blue]), and GL7+ GCs (blue) (n = 3 mice). **Arrows** indicate occasional colocalization of CD4+ cells from CXCR5$^{-/-}$.KRN-Tg mice and SW$_{HEL}$ B cells in follicular GL7^{+} GCs. Original magnification × 10. **B,** BxN.45.1 mice with or without SW$_{HEL}$ B cells and HEL^{3x}-conjugated sheep red blood cells received CD4+ cells from CXCR5$^{-/-}$.KRN-Tg mice. Clinical arthritis scores were measured over time (left) and anti-GPI IgG1 expression in serum was examined on day 14 after transfer by enzyme-linked immunosorbent assay (right) (n = 5 mice per group). **C,** Percentage of GL7^{high}Fas^{high} B220+ germinal center (GC) B cells in spleens of naive SAP$^{+/-}$.A$^{g7+/-}$ mice and their SAP$^{-/-}$.A$^{g7+/-}$ littermates as determined by FACS analysis (n = 4–5 mice per group). **D,** Transfer of CD4+ cells from CXCR5$^{-/-}$ KRN-Tg mice into SAP$^{-/-}$.A$^{g7+/-}$ mice with or without Freund's complete adjuvant (CFA) (n = 5 mice per group). Top, Percentage of GL7^{high}Fas^{high} on B220+ B cells 8 days days after transfer, as determined by FACS analysis. Bottom, Anti-GPI IgG1 expression on day 14 after transfer, as determined by enzyme-linked immunosorbent assay (left), and clinical arthritis scores measured over 28 days (right). Values are the mean ± SD. ** = $P < 0.01$. See Figure 1 for other definitions.

gained access to follicular GCs, these cells were transferred with CD4+ cells from CD45.1^{+}CXCR5$^{-/-}$.KRN-Tg mice into CFA-boosted CD45.1^{+}CD28$^{-/-}$.A$^{g7+/-}$ mouse recipients. Immunohistochemial analysis of spleens collected 8 days after transfer showed that the majority of transferred noncognate CD4+ cells from CD28$^{+/+}$.A$^{g7+/-}$ mice were in the T cell zone; only very few had—possibly randomly—relocated into follicular GCs (Figure 5C).

In summary, ICOS expression is increased on CD28-sufficient CD4+ cells and is increased by CFA-induced inflammation. We speculate that ICOS–ICOSL interactions may be involved in bystander effects mediated by noncognate CD4+ cells; this notion will be interesting to address in future studies and requires ICOS-deficient and ICOSL-deficient mice. It will also be interesting to determine whether noncognate CD4+ bystander cell help occurs outside and/or inside GCs and B cell follicles.

Rare access of CD4+ cells from CXCR5$^{-/-}$.KRN-Tg mice to GCs of an unrelated specificity. Apart from having a hyporesponsive CD4+ cell compartment, CD28$^{-/-}$ mice also exhibited a near complete lack of background GCs (Figure 4A). We therefore sought to

determine whether this could be an additional explanation for the observed deficiency of CD4+ cells from $CXCR5^{-/-}$. KRN-Tg mice to induce a sufficient autoreactive B cell response and disease in $CD28^{-/-}$ mouse recipients. The idea behind this was that preexisting unrelated GC reactions could co-opt autoreactive $CXCR5^{-/-}$ CD4+ cells when paired up physically with cognate B cells, to join a GC reaction of another specificity and exploit this environment for its own purpose.

To examine such a concept, we chose the following consecutive transfer and immunization strategy (Figure 6A): first, we injected CD45.1+ anti-HEL SW_{HEL} B cells into $CD45.1^{+}$BxN.45.1 mice followed by immunization with SRBCs conjugated to mutant HEL^{3x} proteins that bind the SW_{HEL} B cell receptor with low affinity and are primarily directed to GCs (23). Because HEL-specific GC formation can be expected from day 4 onward (22), we chose this time point to inject CD4+ cells from $CD45.2^{+}CXCR5^{-/-}$.KRN-Tg mice and collected spleens for immunohistologic analysis 8 days later. CD4+ cells from $CXCR5^{-/-}$.KRN-Tg mice were identified as CD45.2+, and SW_{HEL} B cells were identified as HEL-binding cells. Thus, we detected only occasional colocalization of CD4+ cells from $CXCR5^{-/-}$. KRN-Tg mice and SW_{HEL} B cells in follicular GL7+ GCs (Figure 6A). Moreover, the cotransfer strategy did not increase anti-GPI IgG1 or the arthritis score compared with transfer of only CD4+ cells from $CXCR5^{-/-}$.KRN-Tg mice (Figure 6B).

To further examine a possible influence of background GCs, CD4+ cells from $CXCR5^{-/-}$.KRN-Tg mice were transferred into $SAP^{-/-}.A^{g7+/-}$ mice, which are unable to create GCs and thus also lack background GCs (Figure 6C). The observation that CFA treatment in $SAP^{-/-}.A^{g7+/-}$ mice that received CD4+ cells from $CXCR5^{-/-}$.KRN-Tg mice could restore autoantibody production, disease, and GCs (Figure 6D) provides further evidence against the notion that background GCs support autoimmunity by co-opting autoaggressive CD4+ cells. Instead, CFA fosters the induction of de novo GCs as a venue for autoantibody production, which then precipitates autoimmunity.

DISCUSSION

In the current study, we used a simple model of autoreactive arthritis-inducing T cell transfer to investigate the mechanisms that lead to antibody-mediated autoimmunity. We resolved the question of whether CXCR5 expression on CD4+ cells is required for their entry into GCs and help for (auto)antibody production (a subject that has been controversial) (12,15–17). We clarify the relevance of bona fide CXCR5+ Tfh cells for optimal GC formation, autoantibody production, and disease development. Their function was, however, not absolute and could be substituted in the presence of sufficient levels of inflammation and noncognate CD4+ cell bystander effects. Moreover, we examined the influence of unrelated background GCs. Our data do not support the concept that ongoing GC reactions may co-opt unrelated CD4+ cells and induce autoimmunity.

The complete abrogation of the autoaggressive B cell response using SAP-deficient self-reactive CD4+ cells from KRN-Tg mice underlines the requirement of long-lasting T cell–B cell interactions (9,10) and GC formation (12) for autoantibody production and arthritis induction. In contrast, CXCR5 expression on CD4+ cells was not vital; nevertheless, bona fide CXCR5+ Tfh cells were necessary to support a GC reaction of maximal magnitude. It is possible that in normal or autoimmune GC reactions, CXCR5− CD4+ cells do get recruited, potentially through their coupling with CXCR5+ B cells. The observation that CXCR5 deficiency in autoreactive antigen-specific CD4+ cells only mildly affected the GC response in WT mouse recipients, while the latter was almost completely abrogated in $CD28^{-/-}$ mouse recipients but restored by adjuvant CFA, shows how multiple factors work in tandem to shape the outcome of a GC response. The clinical relevance for that (i.e., multiple factors work in tandem) is reflected in studies of the association between infections or other environmental factors and autoimmunity (37–39). We assume that such environmental factors may also differ between animal facilities and partly explain the incongruity between studies investigating the importance of CXCR5 on CD4+ cells for GC formation and antibody secretion (12,15–17).

Additionally, varied genetic backgrounds may play a role (e.g., SLAM family sequence polymorphisms that alter susceptibility to autoimmunity). The SLAM family includes 9 proteins that are expressed as costimulatory molecules on various immune cells and modulate their activity, function, and differentiation (40–43). In humans, SLAM locus polymorphisms were shown to correlate with increased susceptibility to systemic lupus erythematosus and RA (44,45). In mice, 2 stable haplotypes of this locus were identified: haplotype 1, which is represented by C57BL/6 mice, and haplotype 2, which is represented by autoimmune-prone strains such as NZB/NZW or NOD/Lt mice. Generally, haplotype 2–associated susceptibility alleles drive autoimmunity when they are present in combination with polymorphic genes in the C57BL/6 genome (43,46,47). In our study, background differences in $A^{g7+/-}$ mice (recipients) are unlikely to influence arthritis development. Moreover, the mutant/gene-

targeted mice used in our study were on a pure C57BL/6 background, which should exclude an autoimmune phenotype due to SLAM locus transfer from 129v to a C57BL/6 background.

We speculate that CD4+ cell bystander effects and ICOS signaling are likely important molecular mechanisms, because they were reduced in $CD28^{-/-}$ mice and boosted by CFA. In accordance with our data, a recent study showed that activated noncognate CD4+ cells triggered GC formation and autoantibody production (27). Also, ICOS expression is sustained in chronic autoinflammatory conditions (33,35,48). The importance of ICOS for the development of GCs (49–51) and Tfh cell differentiation (9,52) has been demonstrated in numerous studies. Additionally, a novel role for ICOS was recently observed. Xu et al reported that developing Tfh cells require ICOSL signals from bystander B cells that do not present antigen but collectively form an ICOS-engaging field for their follicular recruitment (30). Similarly, it appears possible that increased ICOS provision by noncognate T cells may favor an ICOS-engaging field and trigger autoimmunity by increasing the motility of self-reactive B cells and T cells toward B cell follicles. Such a concept is intriguing but requires further studies, ideally using ICOSL and ICOS deficiency in the endogenous and/or antigen-specific T cell compartment.

The mechanisms of action of CFA are versatile and likely to exceed the effects on bystander CD4+ cell activation and ICOS expression, as described above. CFA induces an inflammatory environment by promoting accumulation, expansion, and activation of cells involved in innate and adaptive immunity and a release of inflammatory cytokines (39,53) that may exert triggering effects. In the current study, CFA also increased the critical mass of autoreactive CD4+ cells from $CXCR5^{-/-}$.KRN-Tg mice in lymphoid organs. The mechanism(s) remain unclear, and ICOS–ICOSL effects may play a role. An additional important role was recently attributed to interferon-γ (IFNγ) in CFA-dependent disease models (54), because IFNγ excess leads to pathogenic accumulation of Tfh cells and GCs in lupus (55). Moreover, CFA strongly stimulates antigen-presenting cells, which may trigger activation and expansion of transferred autoreactive cells and support their entry into follicular GCs by CCR7 down-regulation. GC formation may also be alleviated by CFA through stimulatory effects on B cells, mediated in an extrinsic manner (inflammatory cytokines) and/or an intrinsic manner (Toll-like receptor stimulation).

We also examined a potential contribution of unrelated background GCs that may arise from constant exposure of the organism to environmental stimuli. Our theory was that CXCR5-deficient CD4+ cells, when paired with leading cognate B cells (15,16,56), could colonize unrelated preexisting GCs and thereby overcome their intrinsic migration defects and obviate the requirement to reconstruct a new GC environment. An implication would be that animals with many more GCs, perhaps as a result of ongoing infections, would be more likely to support T cell–B cell conjugates and full GC reactions. The results of two-photon laser-scanning microscopy studies of GC dynamics (57,58) support such a model. In these studies, GCs are described as open structures that are continuously patrolled by B cells scanning for cognate antigens trapped on FDCs. B cells with a competitive advantage in antigen-binding affinity could join a preexisting GC (58). Moreover, the plastic environment of GCs could be "hijacked" by heterologous T cell or B cell specificities that are unrelated to the original evoking antigen (57,59). Importantly, invasion was most efficient when T cell help was shared by different heterologous immune responses (57). Such a concept appeared intriguing, but our results did not support it. It must also be considered that in principle the opposite scenario seems possible, i.e., that preexisting GCs hinder rather than facilitate the development of new GCs. Accordingly, in certain experimental models of autoimmunity, microbial stimuli are indispensable for disease development, whereas in other models disease is enhanced by a germ-free environment (60).

In summary, we demonstrate that the outcome of an autoreactive GC response depends not only on the quality and quantity of cognate CD4+ cell help but also on different external influences. Therefore, in the future it will be necessary to determine environmental stimuli and evaluate their contributions to the initiation and perpetuation of autoimmunity. Special attention must be paid to the use of immunization strategies and adjuvants. Although use of adjuvants is common, little is known about the exact mechanism of action. In individuals with an adverse genetic makeup, the immune stimulatory effects of adjuvants may promote autoimmunity.

ACKNOWLEDGMENTS

We thank D. Mathis and C. Benoist for providing KRN-transgenic mice and S. Tangye for providing $SAP^{-/-}$ mice. We also thank the staff at the Garvan Flow Cytometry Facility and the Monash Flow Cytometry Facility (Flowcore) for assisting with cell sorting, as well as the staff at Australian BioResources. We are grateful to the Garvan Australian Cancer Research Foundation facility (ACRF) for assisting with genotyping, the Monash Histology Facility for assisting with preparation of tissue sections, and the Monash Micro Imaging (MMI) facility for providing instrumentation, training, and general support. Finally, we thank Dietmar Pfeifer, PhD (Geno-

mics Facility, Department of Hematology and Oncology, University Freiburg Medical Centre) for helpful discussions and advice.

AUTHOR CONTRIBUTIONS

All authors were involved in drafting the article or revising it critically for important intellectual content, and all authors approved the final version to be published. Dr. Chevalier had full access to all of the data in the study and takes responsibility for the integrity of the data and the accuracy of the data analysis.

Study conception and design. Chevalier, Macia, Thorburn, Tsai, Brink, Yu, Mackay.

Acquisition of data. Chevalier, Tan, Mason, Robert, Thorburn, Wong, Bourne, Yu, Mackay.

Analysis and interpretation of data. Chevalier, Mason, Robert, Thorburn, Wong, Brink, Yu, Mackay.

ADDITIONAL DISCLOSURES

Author Mackay is an employee of Pfizer.

REFERENCES

1. Vinuesa CG, Sanz I, Cook MC. Dysregulation of germinal centres in autoimmune disease. Nat Rev Immunol 2009;9:845–57.
2. Vinuesa CG, Tangye SG, Moser B, Mackay CR. Follicular B helper T cells in antibody responses and autoimmunity. Nat Rev Immunol 2005;5:853–65.
3. Chtanova T, Tangye SG, Newton R, Frank N, Hodge MR, Rolph MS, et al. T follicular helper cells express a distinctive transcriptional profile, reflecting their role as non-Th1/Th2 effector cells that provide help for B cells. J Immunol 2004;173:68–78.
4. King C, Tangye SG, Mackay CR. T follicular helper (TFH) cells in normal and dysregulated immune responses. Ann Rev Immunol 2008;26:741–66.
5. Schaerli P, Willimann K, Lang AB, Lipp M, Loetscher P, Moser B. CXC chemokine receptor 5 expression defines follicular homing T cells with B cell helper function. J Exp Med 2000;192:1553–62.
6. Breitfeld D, Ohl L, Kremmer E, Ellwart J, Sallusto F, Lipp M, et al. Follicular B helper T cells express CXC chemokine receptor 5, localize to B cell follicles, and support immunoglobulin production. J Exp Med 2000;192:1545–52.
7. Ansel KM, McHeyzer-Williams LJ, Ngo VN, McHeyzer-Williams MG, Cyster JG. In vivo-activated CD4 T cells upregulate CXC chemokine receptor 5 and reprogram their response to lymphoid chemokines. J Exp Med 1999;190:1123–34.
8. Chevalier N, Jarrossay D, Ho E, Avery DT, Ma CS, Yu D, et al. CXCR5 expressing human central memory CD4 T cells and their relevance for humoral immune responses. J Immunol 2011;186:5556–68.
9. Crotty S, Kersh EN, Cannons J, Schwartzberg PL, Ahmed R. SAP is required for generating long-term humoral immunity. Nature 2003;421:282–7.
10. Qi H, Cannons JL, Klauschen F, Schwartzberg PL, Germain RN. SAP-controlled T-B cell interactions underlie germinal centre formation. Nature 2008;455:764–9.
11. Han S, Cao S, Bheekha-Escura R, Zheng B. Germinal center reaction in the joints of mice with collagen-induced arthritis: an animal model of lymphocyte activation and differentiation in arthritis joints. Arthritis Rheum 2001;44:1438–43.
12. Victoratos P, Kollias G. Induction of autoantibody-mediated spontaneous arthritis critically depends on follicular dendritic cells. Immunity 2009;30:130–42.
13. Wu HJ, Ivanov II, Darce J, Hattori K, Shima T, Umesaki Y, et al. Gut-residing segmented filamentous bacteria drive autoimmune arthritis via T helper 17 cells. Immunity 2010;32:815–27.
14. Keszei M, Detre C, Castro W, Magelky E, O'Keeffe M, Kis-Toth K, et al. Expansion of an osteopontin-expressing T follicular helper cell subset correlates with autoimmunity in B6.Sle1b mice and is suppressed by the H1-isoform of the Slamf6 receptor. FASEB J 2013;27:3123–31.
15. Arnold CN, Campbell DJ, Lipp M, Butcher EC. The germinal center response is impaired in the absence of T cell-expressed CXCR5. Eur J Immunol 2007;37:100–9.
16. Haynes NM, Allen CD, Lesley R, Ansel KM, Killeen N, Cyster JG. Role of CXCR5 and CCR7 in follicular Th cell positioning and appearance of a programmed cell death gene-1^{high} germinal center-associated subpopulation. J Immunol 2007;179:5099–108.
17. Hardtke S, Ohl L, Forster R. Balanced expression of CXCR5 and CCR7 on follicular T helper cells determines their transient positioning to lymph node follicles and is essential for efficient B-cell help. Blood 2005;106:1924–31.
18. Moriyama S, Takahashi N, Green JA, Hori S, Kubo M, Cyster JG, et al. Sphingosine-1-phosphate receptor 2 is critical for follicular helper T cell retention in germinal centers. J Exp Med 2014;211:1297–305.
19. Selmi C, Lu Q, Humble MC. Heritability versus the role of the environment in autoimmunity. J Autoimmun 2012;39:249–52.
20. Chevalier N, Thorburn AN, Macia L, Tan J, Juglair L, Yagita H, et al. Inflammation and lymphopenia trigger autoimmunity by suppression of IL-2-controlled regulatory T cell and increase of IL-21-mediated effector T cell expansion. J Immunol 2014;193:4845–58.
21. Tai X, Cowan M, Feigenbaum L, Singer A. CD28 costimulation of developing thymocytes induces Foxp3 expression and regulatory T cell differentiation independently of interleukin 2. Nat Immunol 2005;6:152–62.
22. Chan TD, Gatto D, Wood K, Camidge T, Basten A, Brink R. Antigen affinity controls rapid T-dependent antibody production by driving the expansion rather than the differentiation or extrafollicular migration of early plasmablasts. J Immunol 2009;183:3139–49.
23. Paus D, Phan TG, Chan TD, Gardam S, Basten A, Brink R. Antigen recognition strength regulates the choice between extrafollicular plasma cell and germinal center B cell differentiation. J Exp Med 2006;203:1081–91.
24. Korganow AS, Ji H, Mangialaio S, Duchatelle V, Pelanda R, Martin T, et al. From systemic T cell self-reactivity to organ-specific autoimmune disease via immunoglobulins. Immunity 1999;10:451–61.
25. Matsumoto I, Staub A, Benoist C, Mathis D. Arthritis provoked by linked T and B cell recognition of a glycolytic enzyme. Science 1999;286:1732–5.
26. Jacobs JP, Wu HJ, Benoist C, Mathis D. IL-17-producing T cells can augment autoantibody-induced arthritis. Proc Nat Acad Sci U S A 2009;106:21789–94.
27. Banczyk D, Kalies K, Nachbar L, Bergmann L, Schmidt P, Bode U, et al. Activated CD4+ T cells enter the splenic T-cell zone and induce autoantibody-producing germinal centers through bystander activation. Eur J Immunol 2014;44:93–102.
28. Shahinian A, Pfeffer K, Lee KP, Kundig TM, Kishihara K, Wakeham A, et al. Differential T cell costimulatory requirements in CD28-deficient mice. Science 1993;261:609–12.
29. Ferguson SE, Han S, Kelsoe G, Thompson CB. CD28 is required for germinal center formation. J Immunol 1996;156:4576–81.
30. Xu H, Li X, Liu D, Li J, Zhang X, Chen X, et al. Follicular T-helper cell recruitment governed by bystander B cells and ICOS-driven motility. Nature 2013;496:523–7.
31. Mak TW, Shahinian A, Yoshinaga SK, Wakeham A, Boucher LM, Pintilie M, et al. Costimulation through the inducible costimulator ligand is essential for both T helper and B cell functions in T cell-dependent B cell responses. Nat Immunol 2003;4:765–72.

32. Hu YL, Metz DP, Chung J, Siu G, Zhang M. B7RP-1 blockade ameliorates autoimmunity through regulation of follicular helper T cells. J Immunol 2009;182:1421–8.
33. Iwai H, Kozono Y, Hirose S, Akiba H, Yagita H, Okumura K, et al. Amelioration of collagen-induced arthritis by blockade of inducible costimulator-B7 homologous protein costimulation. J Immunol 2002;169:4332–9.
34. Frey O, Meisel J, Hutloff A, Bonhagen K, Bruns L, Kroczek RA, et al. Inducible costimulator (ICOS) blockade inhibits accumulation of polyfunctional T helper 1/T helper 17 cells and mitigates autoimmune arthritis. Ann Rheum Dis 2010;69:1495–501.
35. Rottman JB, Smith T, Tonra JR, Ganley K, Bloom T, Silva R, et al. The costimulatory molecule ICOS plays an important role in the immunopathogenesis of EAE. Nat Immunol 2001;2:605–11.
36. Vinuesa CG, Cook MC, Angelucci C, Athanasopoulos V, Rui L, Hill KM, et al. A RING-type ubiquitin ligase family member required to repress follicular helper T cells and autoimmunity. Nature 2005;435:452–8.
37. Sfriso P, Ghirardello A, Botsios C, Tonon M, Zen M, Bassi N, et al. Infections and autoimmunity: the multifaceted relationship. J Leukoc Biol 2010;87:385–95.
38. Doria A, Sarzi-Puttini P, Shoenfeld Y. Infections, rheumatism and autoimmunity: the conflicting relationship between humans and their environment. Autoimmun Rev 2008;8:1–4.
39. Billiau A, Matthys P. Modes of action of Freund's adjuvants in experimental models of autoimmune diseases. J Leukoc Biol 2001;70:849–60.
40. Calpe S, Wang N, Romero X, Berger SB, Lanyi A, Engel P, et al. The SLAM and SAP gene families control innate and adaptive immune responses. Adv Immunol 2008;97:177–250.
41. Cannons JL, Tangye SG, Schwartzberg PL. SLAM family receptors and SAP adaptors in immunity. Ann Rev Immunol 2011;29: 665–705.
42. Detre C, Keszei M, Garrido-Mesa N, Kis-Toth K, Castro W, Agyemang AF, et al. SAP expression in invariant NKT cells is required for cognate help to support B-cell responses. Blood 2012;120:122–9.
43. Detre C, Keszei M, Romero X, Tsokos GC, Terhorst C. SLAM family receptors and the SLAM-associated protein (SAP) modulate T cell functions. Sem Immunopathol 2010;32:157–71.
44. Cunninghame Graham DS, Vyse TJ, Fortin PR, Montpetit A, Cai YC, Lim S, et al. Association of LY9 in UK and Canadian SLE families. Genes Immun 2008;9:93–102.
45. Suzuki A, Yamada R, Kochi Y, Sawada T, Okada Y, Matsuda K, et al. Functional SNPs in CD244 increase the risk of rheumatoid arthritis in a Japanese population. Nat Genet 2008;40: 1224–9.
46. Wandstrat AE, Nguyen C, Limaye N, Chan AY, Subramanian S, Tian XH, et al. Association of extensive polymorphisms in the SLAM/CD2 gene cluster with murine lupus. Immunity 2004;21: 769–80.
47. Keszei M, Detre C, Rietdijk ST, Munoz P, Romero X, Berger SB, et al. A novel isoform of the Ly108 gene ameliorates murine lupus. J Exp Med 2011;208:811–22.
48. Iwai H, Abe M, Hirose S, Tsushima F, Tezuka K, Akiba H, et al. Involvement of inducible costimulator-B7 homologous protein costimulatory pathway in murine lupus nephritis. J Immunol 2003;171:2848–54.
49. Dong C, Temann UA, Flavell RA. Cutting edge: critical role of inducible costimulator in germinal center reactions. J Immunol 2001;166:3659–62.
50. Tafuri A, Shahinian A, Bladt F, Yoshinaga SK, Jordana M, Wakeham A, et al. ICOS is essential for effective T-helper-cell responses. Nature 2001;409:105–9.
51. McAdam AJ, Greenwald RJ, Levin MA, Chernova T, Malenkovich N, Ling V, et al. ICOS is critical for CD40-mediated antibody class switching. Nature 2001;409:102–5.
52. Bauquet AT, Jin H, Paterson AM, Mitsdoerffer M, Ho IC, Sharpe AH, et al. The costimulatory molecule ICOS regulates the expression of c-Maf and IL-21 in the development of follicular T helper cells and TH-17 cells. Nat Immunol 2009;1:167–75.
53. Rose NR. Autoimmunity, infection and adjuvants. Lupus 2010; 19:354–8.
54. Matthys P, Vermeire K, Heremans H, Billiau A. The protective effect of IFN-γ in experimental autoimmune diseases: a central role of mycobacterial adjuvant-induced myelopoiesis. J Leukoc Biol 2000;68:447–54.
55. Lee SK, Silva DG, Martin JL, Pratama A, Hu X, Chang PP, et al. Interferon-γ excess leads to pathogenic accumulation of follicular helper T cells and germinal centers. Immunity 2012;37: 880–92.
56. Okada T, Miller MJ, Parker I, Krummel MF, Neighbors M, Hartley SB, et al. Antigen-engaged B cells undergo chemotaxis toward the T zone and form motile conjugates with helper T cells. PLoS biology 2005;3:e150.
57. Schwickert TA, Alabyev B, Manser T, Nussenzweig MC. Germinal center reutilization by newly activated B cells. J Exp Med 2009;206:2907–14.
58. Schwickert TA, Lindquist RL, Shakhar G, Livshits G, Skokos D, Kosco-Vilbois MH, et al. In vivo imaging of germinal centres reveals a dynamic open structure. Nature 2007;446:83–7.
59. Casola S, Otipoby KL, Alimzhanov M, Humme S, Uyttersprot N, Kutok JL, et al. B cell receptor signal strength determines B cell fate. Nat Immunol 2004;5:317–27.
60. Pasztoi M, Misjak P, Gyorgy B, Aradi B, Szabo TG, Szanto B, et al. Infection and autoimmunity: lessons of animal models. Eur J Microbiol Immunol 2011;1:198–207.